Optimization of Deployable Base Stations With Guaranteed QoE in Disaster Scenarios

Junbo Wang, *Member, IEEE*, Song Guo, *Senior Member, IEEE*, Zixue Cheng, *Member, IEEE*,
Peng Li, *Member, IEEE*, and Jie Wu, *Fellow, IEEE*

Abstract—Reconstructing emergency communication networks (ECNs) quickly after a disaster occurs is critical so that people can share information and confirm their safety. In recent studies, deployable base stations (DBSs) have demonstrated their ability to reconstruct an ECN. However, considering limited resources, it is impossible to deploy DBSs in the whole disaster area. The above shortage can be covered by deploying small-cell networks (i.e., low-power transmission base stations) in areas with high communication demand, e.g., in refuges. Considering the above two-tier ECN, in this paper, we study its performance and optimization issue with the objective of minimizing the number/density of DBSs while guaranteeing acceptable coverage probabilities for both communication tiers. The majority of current research focuses on scenarios where the base stations follow a homogeneous Poisson point process of coverage probability. It is difficult to transfer the results to other applications, e.g., when communication resources are shared, such as by refugees following a disaster. In such cases, the distribution of users is closer to that of a Poisson cluster process. We then investigate the optimization method to minimize the number/density of DBSs. We used Monte Carlo methods with various parameter choices to evaluate the results and to determine the accuracy of our evaluation.

Index Terms—Anti-disaster network, association probability, coverage probability, heterogeneous emergency communication networks (ECNs), Poisson cluster process (PCP).

I. INTRODUCTION

THE communication network is crucially important in a disaster, since both rescue and recovery greatly depend on the provided communication channels. However, the conventional communication network is fragile once a disaster happens. A temporal communication system, namely, an emergency communication network (ECN), must be quickly constructed to connect users.

Deployable base station (DBS)-based ECNs have shown possible applications for supporting communication after a disaster, e.g., NTT Japan has proposed a DBS to be deployed after a disaster occurs. Users can use the DBS to send messages from a disaster area [1]. However, effectively deploying them is still an ongoing research problem, since it is impossible to deploy DBSs in the entire disaster area.

On the other hand, multitier heterogeneous cellular networks (HCNs) have demonstrated their ability to enhance the coverage of communication networks. For example, femtocell base stations (BSs) can be deployed in houses near the edges of macrocell coverage in order to support users who require high-speed data transmission services.

Similar to HCNs, small-cell networks can support coverage of DBSs especially in areas with high communication demand, e.g., in refuges, by constructing a two-tier heterogeneous ECN. The first tier is a macrocell tier composed of DBSs, which can provide communication services with a relatively long distance, similar to macrocell BSs in a cellular communication system. The second tier is composed of small-cell BSs, deployed in shelters. The advantages to construct such a heterogeneous ECN include the following: 1) it is possible to provide communication services for a crowd of users in a shelter and 2) deployment of DBSs in a disaster area can quickly reconstruct a communication network and cover a large area, while it is impractical for deploying small-cell BSs in a large-scale area.

In such a two-tier heterogeneous ECN, one of the key research issues is the minimization of communication resources, e.g., the number/density of DBSs, while guaranteeing coverage probabilities for both communication tiers, considering limited communication resource in a disaster scenario. For example, generally, DBSs should be transferred from other areas, and the process will take time. In this paper, we take the above research problem and study the performance and optimization issue with the objective of minimizing number/density of DBSs.

Coverage probability, which is the likelihood that users will have acceptable service is of utmost importance to HCNs. The results of determining the coverage probability can be used as a basis for other applications, such as improving access mechanisms [2]–[4] or optimizing an HCN.

Existing studies of coverage (alternatively, outage) probability can be categorized as mathematical analyses [5] or performance evaluations [6]–[8]. However, almost all of the research has assumed that the BSs follow a homogeneous Poisson point process (PPP) distribution. In contrast, in a disaster scenario, when communication services are not generally available, people tend to gather in shelters. In such a situation, it is difficult
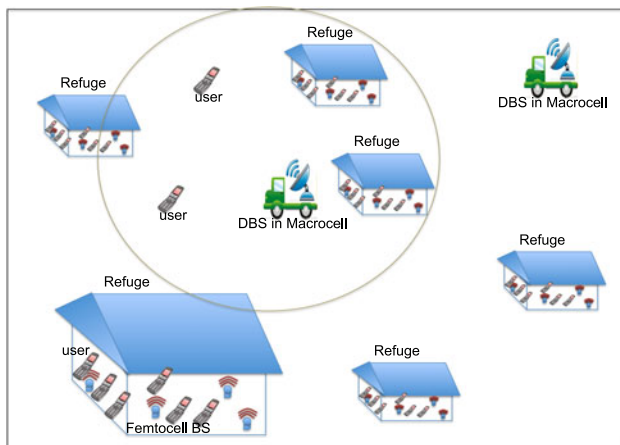
Fig. 1. Model of this application.

to ensure an acceptable level of service, since the bandwidth is shared with a large group, however the deployment of femtocell BSs can enhance the service, as shown in Fig. 1, through the following ways.

1) Deployment of femtocell BSs in a refuge can provide more communication resources to meet requirements from a crowd of users.
2) Deployment of femtocell BSs in the communication edge of macrocell BS can enable a stable and smooth communiation.

Based on the issues described above, in this paper, we consider the coverage probability of small-cell BSs that follow a Poisson cluster process (PCP). After disaster occurrence, most of those affected would like to leave home [9] and stay at a refuge for safety and information acquisition. Distribution of the refuges can be represented as a PPP distribution, and, for each refuge, a cluster of femtocell BSs can be deployed. The above scenario mostly matches with the definition of PCP [10].

Although this is an emerging topic, there has already been a study [11] that evaluates the coverage probability for a PCP; it presents a mathematical analysis of the coverage probability when there is one macrocell BS and the distance between the user and the BS is known *a priori*. However, in most cases, the distance is not known, and we want to know the coverage probability for a random user in the network, and in this particular case, we are primarily interested in the conditional probability of coverage when the user is inside a given cluster. This is because in such a scenario, the small-cell BSs will follow a PCP, and most of the users will remain within a cluster. For this reason, it will be more meaningful and will have more applications if we determine the conditional probability of coverage for users within clusters.

To guarantee QoE, we consider both the conditional association probability and the conditional coverage probability for users who remain within a cluster and access a two-tier ECN. The "condition" stated in the paper is to represent "on the condition that the user is staying inside of a refuge" to have more applications and possible users. The first tier is a macrocell (i.e., DBS tier), and the second tier is a small cell, which can be either a femtocell or a picocell, depending on the particular application.

The macrocell is to provide a long-distance communication. Small cell, e.g., femtocell or picocell, provides communication services for a shorter distance. Femtocell BS can be deployed at home environment to enhance communication services for residents, while picocell BS is deployed in a larger area, e.g., factory. In this paper, for simplicity, we assume that the small cell is a femtocell; however, the results can be generalized to picocells.

More specifically, first we consider the conditional association probability. Here, association refers to the communication tier that serves a given user, and this is based on the power received at the user's location from the BSs in the different tiers. This probability is based on the distributions of BSs in a given scenario; in this paper, we assume that the DBSs in macrocell follow a homogeneous PPP and the small-cell BSs follow a PCP.

Next, we consider the conditional coverage probability for a user within a cluster. Coverage at a particular location (e.g., the user) is defined to occur when the signal-to-interference-and-noise ratio (SINR) from a given BS is greater than a given threshold. The probability of this occurrence is based on the distribution of macrocell and small-cell BSs. Finally, we have achieved approximate theoretical upper bound of conditional coverage probabilities for both tiers.

Then, we study the optimization issue to minimize the density of the macrocell DBS, taking the conditional coverage probabilities as constraints. The reason why we are taking the conditional coverage probabilities as constraints is to guarantee the performance of the communication network.

Finally, we perform a comprehensive evaluation, based on Monte Carlo methods. We simulate a network environment in which DBSs in a macrocell follow a homogeneous PPP and small-cell BSs follow a PCP within a given area. In repeated Monte Carlo trials, for a random user within a cluster, we calculate the corresponding SINR from the serving BS and evaluate the probability of coverage. These results are critical for evaluating the accuracy of the analytical results in this paper. Furthermore, we evaluate the performance of such a communication network for various values of the network parameters, such as the density of the distribution of macrocell and small-cell BSs. These results will be useful for the design of future communication networks. And finally, we have evaluated the performance of the proposed optimization method.

The main contributions of the paper can be summarized as follows.

1) Mathematical analysis and evaluation of the conditional association probability and conditional coverage probability for a heterogeneous ECN: we present the equations and the detailed derivations for these two probabilities and show how they depend on the features of the PCP.
2) Optimization of number/density of macrocell DBSs, while guaranteeing the conditional coverage probability: we formularize the problem but the challenging issue here is that the final expression of the conditional probability is so complex that it does not have a close-form expression. In this paper, we take a numerical fitting approach to solve it.
3) A numerical study based on a Monte Carlo method, and a performance evaluation based on various values of the

network parameters, such as the density of the distribution of the macrocell and femtocell BSs.

The remainder of this paper is organized as follows. In Section II, we review the important related literature. In Section III, we present the system and network models and then formularize the optimization problem. In Sections IV and V, we analyze the conditional association probability and the conditional coverage probability, respectively. In Section VI, we solve the optimization problem, and the evaluation results are presented in Section VII. Finally, we present our conclusions in Section VIII.

II. RELATED WORKS

The literature considering the coverage probability in HCNs can be categorized as follows: 1) mathematical analyses and 2) evaluations of applications. These will be discussed separately below.

A. Deployment of DBSs

Useful metrics have been proposed to evaluate the deployment of DBSs, e.g., coverage, connectivity and energy [12]–[15]. Robinson and Knightly [12] studied the coverage problem of a DBS and showed that random deployment needs more nodes to achieve the same coverage target. A hexagonal grid topology results in more coverage dead spots than a square or triangular grid. Furthermore, Fu *et al.* [13] investigated the energy of DBSs to maintain the connectivity of deployed DBSs. On the other hand, some coverage control methods have been proposed for mobile mesh networks. For example, Cortes *et al.* [16] presented a set of control and coordination algorithms for optimization of the location of vehicles. Mahboubi *et al.* [17] proposed some distributed deployment strategies with a prioritized sensing field. However, no research has examined the optimal density of DBS considering a two-tier heterogeneous ECN, with detailed mathematic analyses of coverage probability to a random user.

B. Mathematical Analyses of Coverage Probability

Mathematical analyses of coverage probability have primarily been based on either of two models. The first assumes that the BSs are distributed as a hexagonal grid; this approach has been used in industry and academia [18]–[20]. However, it is difficult to create this distribution, and the calculated probability cannot be generalized to a more realistic situation [5], [21]. The other approach is to model the deployment of BSs as random points obtained from a spatial stochastic process, such as a PPP. Such an approach has been shown to be as accurate as the grid model [18], [22], but it is suitable only for small-cell networks, due to the unknown and unplanned positions of the BSs.

Several studies have analyzed the coverage probability of BSs distributed according to a PPP. Dhillon *et al.* [5] mathematically analyzed a *K*-tier downlink HCN while considering both open- and closed-access policies, and their results can be efficiently adopted by service providers [23]. The coverage probability with biased cell associations has also been considered [18], [24], [25].

Flexible cell associations can result in a better allocation of communication resources, since mobile users in an overloaded tier can be transferred to one with a lighter load [24]. The benefits of adding more small-cell BSs to areas with poor coverage have been considered for networks of small-cell BSs that are nonuniformly distributed [26]. In addition, the performance of HCNs has been evaluated [6]–[8], and the effects of various values of the parameters have been considered; these parameters include the fading channels [27] and the number of sectors [4], [28].

Most studies have assumed that the distribution of small-cell BSs follows a homogeneous PPP, although this is unsuitable for many applications, such as a disaster scenario, as discussed above and as shown in Fig. 1. For this reason, the Monte Carlo method has been used to evaluate the coverage probability of PCPs [11]. However, this approach has the following shortcomings:

1) the results are restricted to cases in which the distance from the user to the macrocell DBS is known, and they cannot be generalized to determine the coverage probability for a user in a random location in the communication network; and

2) the association issue is ignored in the analysis, so the results are not applicable to realistic scenarios, since it is necessary to determine which BS will serve a user prior to initiating communication.

C. Application Study Based on Mathematical Results

A mathematical evaluation of the coverage probability can be adapted to various applications, such as access control mechanisms and the optimization of networks. For example, in order to maximize throughput, a genetic-algorithm-based access control mechanism has been proposed [29], and in order to allow dynamic access of an HCN, an approach based on the Stachelberg model has been proposed [2]. These approaches have been used to design access mechanisms, and the performance of such mechanisms has been evaluated [30]. This approach can also be used to optimize the usage of an HCN [3], [4]. However there is no study on optimization of DBS's density while guaranteeing acceptable coverage probability, considering a PCP distribution of small-cell BSs. Meanwhile, our analytical results will be useful for the further development of efficient access control mechanisms for small-cell networks where the BSs are distributed according to a PCP.

D. PCP for Disaster Scenario

The PCP has been widely applied to studies for disaster. In [31], each earthquake is regarded as a point event, and a stochastic model is developed for earthquake occurrence. Matsui has studied a simple but flexible Poisson cluster model in [32]. Thompson and Guttorp [33] have shown that a Poisson cluster model can better describe data on severe cyclonic storms striking the Bay of Bengal coast during 1877–1977. Meanwhile, A Poisson cluster distribution is adopted to model the victim distribution in [34], which derives a hazard map for earthquake occurrences in Pakistan from a catalog that contains spatial coordinates of shallow earthquakes of magnitude 4.5 or larger aggregated over calendar years. A similar model is also
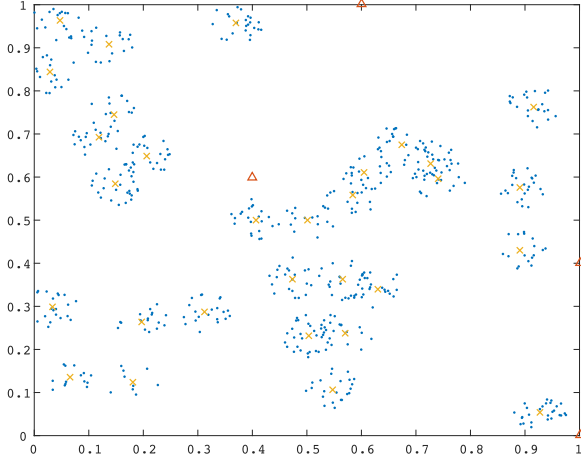
Fig. 2. Example of a cluster process.

Fig. 3. Interference model.

considered in [35]. This paper constructed several space–time statistical models based on classical empirical studies of clustering and some more speculative hypotheses.

III. MODELS

Before presenting our mathematic analysis in detail, we first present the system model that we consider.

A. System Model

In this study, we consider a two-tier ECN that includes both DBSs in macrocell and BSs in femtocell that are located according to random processes. The DBSs in macrocell are distributed according to a homogeneous PPP (denoted as Θ_1 with density λ_1), and the femtocell BSs are distributed according to a PCP (denoted as Θ_f).

Each PCP (Θ_f) is generated by a point process $\Theta_c = (x_1, x_2, \ldots, x_i, \ldots, x_m)$, and each point in Θ_c (each x_i) is said to be a parent point of the PCP. The density of the parent points is denoted as λ_c. Around each parent point, a cluster of points (M_{x_i}) will be created within a range of radius D_c and with a specified density λ_d, and these points will be distributed according to a uniform Poisson distribution. Therefore, Θ_f is a Matern cluster process, which is a special kind of PCP. Note that Θ_f can be represented as

$$\Theta_f = \bigcup_{x_i \in \Theta_c} M_{x_i}. \tag{1}$$

A basic image resulting from a PCP can be seen in Fig. 2, in which the DBSs in macrocell are formulated as Θ_1, a homogeneous PPP with density λ_1 (see the red triangle in Fig. 2). The femtocell BSs generated by Θ_f are shown as blue points, and yellow crosses indicate the parent points. The notation is summarized as follows.

Θ_1 Process generating macrocell DBSs.
λ_1 Density of macrocell DBSs.
Θ_f Process generating femtocell BSs.
Θ_c Process generating parent points.
λ_c Density of parent points.
λ_d Density of femtocell BSs in each cluster.
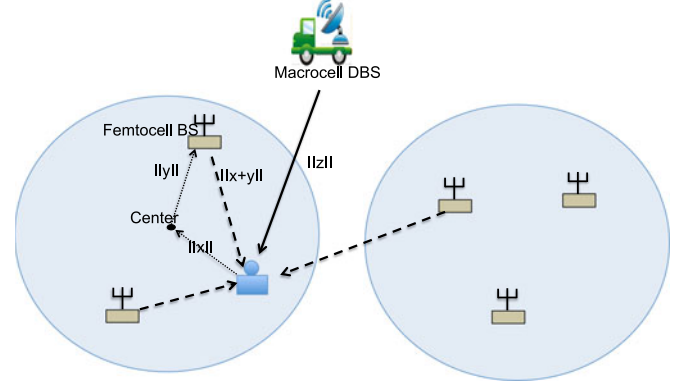D_c Radius of each cluster.

B. Network Model

In this paper, we assume that within each tier, each of the BSs have the same transmission power, which we denote as P^m for the macrocells and P^f for the femtocells. The pass loss is represented in

$$g(d_{kl}) = K_j d_{kl}^{-\alpha^j}. \tag{2}$$

where d_{kl} is denoted as the distance from the user k to the associated BS l. And the user k is served by tier j, while j equals m or f for the macrocell or femtocell tier, respectively.

K_j [11] is a constant to merge constant parameters together. More specifically, SUI (Stanford University Interim) Terrian C model is taken for path loss [36] as

$$\mathrm{PL} = A + 10\gamma \log_{10}(d/d_0) + s. \tag{3}$$

and the constant parameters (e.g., free space loss A, shadowing effect s, carrier frequency loss component, and wall penetration loss) are merged in K_j with a non-dB form.

The power received from tier j at the location of the user k from BS l can be written as

$$p_{kl}^j = P^j h_{kl}^j g(d_{kl}). \tag{4}$$

We considered different values for the pass loss for each tier, i.e., a^m and a^f for the macrocell and femtocell, respectively, and we also considered Rayleigh fading between each user and the serving BS. The impact of fading follows the exponential distribution, i.e., $h \sim \exp(1)$. h_{kl}^j is a general representation of fading parameter in the tier j for the user k with BS l.

Fig. 3 shows the interference model. Here, we assume a typical user within a cluster located around the origin. x, y, and z are points generated in the plane, to represent a center of cluster, a femtocell BS deployed around x, and a macrocell BS. x is a parent point and y is a surrounding point generated based on PCP. z represents a macrocell BS, following a PPP distribution. x and z share the same origin, and the daughter point y takes its parent point x as the origin. Then, based on vector operation, the distance between femtocell BS and a typical user is equal to $\|x + y\|$.

Finally, the SINR for user k served by a BS l in tier j can be written as

$$\text{SINR(k)} = \frac{p_{kl}^j}{I_k^j + \sigma^2} \tag{5}$$

where I_k^j denotes the interference at the user k, and will be studied in Section V for details.

C. Problem Formulation

With the system and network models, we study a density minimization problem, while guaranteeing the communication performance to users. As discussed in Section I, understanding the minimal required DBSs in a disaster area is rather important, considering limited communication resources after occurrence of a disaster. Meanwhile, the optimization should be constrained by the coverage probabilities from both communication tiers, to ensure QoE to users. Then, the problem is formalized as follows.

The Density Minimization Problem (DMP):

Given a group of small-cell BSs deployed randomly following PCP, a group of DBSs deployed randomly following PPP, the goal is to minimize the density of DBS, while guaranteeing acceptable coverage probabilities in both communication tiers, for a random user in a cluster.

The problem can be further formularized as follows:

$$\textbf{DMP}: \qquad \min \ \lambda_1 \qquad \text{subject to:}$$

$$c_{m|\text{in}} \geq \eta_1 \tag{6}$$

$$c_{f|\text{in}} \geq \eta_2 \tag{7}$$

$$P^m \geq P^f, \ 0 < \lambda_1 < 1, \ 0 < \lambda_d < 1 \tag{8}$$

System and Network Models in Sections III-A and III-B.
$$\tag{9}$$

$c_{m|\text{in}}$ and $c_{f|\text{in}}$ denote the conditional coverage probabilities that the user is inside of a refuge, for macrocell and femtocell, respectively. Better QoE for users can be achieved through the constraints (6) and (7). The constraints (8) and (9) are used to reach a reasonable result, with the proposed network model.

Then the further challenging issue is the mathematic expression of $c_{m|\text{in}}$ and $c_{f|\text{in}}$, which will be studied in Sections IV and V for details.

For simplicity, we use the following notation: $P_m^f = \frac{P^m}{P^f}$, $P_f^m = \frac{P^f}{P^m}$, $K_m^f = \frac{K^m}{K^f}$, and $K_f^m = \frac{K^f}{K^m}$, in this paper.

IV. CONDITIONAL ASSOCIATION PROBABILITY AND PROBABILITY DISTRIBUTION FUNCTION

Since the communication system needs to decide which communication tier should serve the user before providing services, conditional association probability is studied first in Section IV.

The conditional association probability is the probability that a user is served by a given BS, given that the user is within a given cluster. Since most of the people would like to leave home [9] and stay at refuges after disaster occurrence, the study can have more possible users.
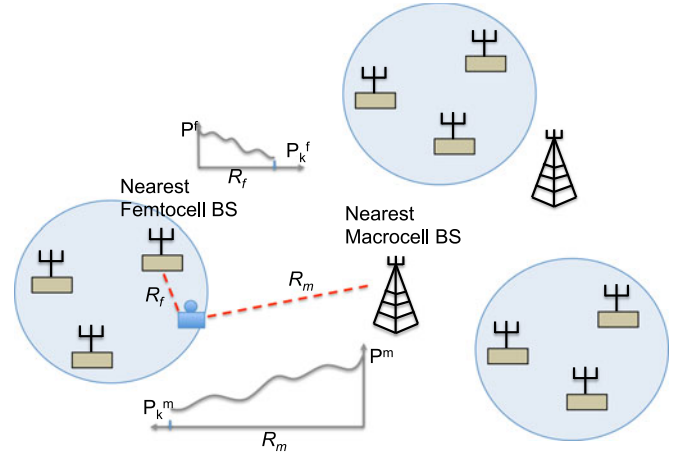

Fig. 4.   Conditional association probability.

We denote the conditional association probability as $A_{j|\text{in}}$, and it depends on the signal power from the BS in each tier that is closest to the user's location, as shown in Fig. 4. j can be replaced by m or f to represent the conditional association probability for macrocell or femtocell tiers, respectively.

$A_{j|\text{in}}$ is defined in

$$A_{f|\text{in}} = \mathbb{P}[u_k \overset{a.s.}{=} j | u_k \in C] = \mathbb{P}[P_k^j > P_k^{j-} | u_k \in C]. \tag{10}$$

where $u_k \overset{a.s.}{=} j$ indicates that the user k is served by the tier j. $u_k \in C$ indicates that the user k is within a cluster/refuge, which is the area with coverage from a group of femtocell BSs [M_{x_i} in (1)], and C is used to represent a cluster/refuge.

Here, P_k^j / P_k^{j-} is denoted as the power received at the user k from the nearest BS in the $j/j-$ communication tier, where the distance from the BS is denoted as R^j / R^{j-}. j or $j-$ can be replaced by m or f for macrocell or femtocell tier, as shown in Fig. 4. Meanwhile, P_k^j and P_k^{j-} are long-term averaged value, so that fading is averaged out, and the results lead to Lemmas 1 and 2.

Lemma 1: The conditional association probability for a macrocell and a user who stays within a cluster is

$$A_{m|\text{in}} = 2\pi\lambda_d \int_0^{D_0} r \exp(-\pi\lambda_d r^2)$$

$$* \left(1 - \exp\left\{-\pi\lambda_1 (P_f^m K_f^m)^{\frac{1}{\alpha^m}} r^{\frac{2\alpha f}{\alpha^m}}\right\}\right) dr \tag{11}$$

where

$$D_0 = \left(\frac{1}{\pi\lambda_d}\right)^{\frac{1}{2}}.$$

Proof: See Appendix A for a detailed derivation.   ∎

Lemma 2: The conditional association probability for a femtocell and a user who stays within a cluster is

$$A_{f|\text{in}} = 2\pi\lambda_d \int_0^{D_0} r \exp(-\pi\lambda_d r^2)$$

$$* \exp\left\{-\pi\lambda_1 (P_f^m K_f^m)^{\frac{1}{\alpha^m}} r^{\frac{2\alpha f}{\alpha^m}}\right\} dr$$

where

$$D_0 = \left(\frac{1}{\pi \lambda_d}\right)^{\frac{1}{2}}.$$

Proof: See Appendix B for a detailed derivation. ∎

Then we change to a preliminary study, i.e., the probability distribution function for the tier j when the user remains within a cluster; which is denoted as $f_{X_{j}|\text{in}}(x)$. j also equals m or f to represent different communication tier. Doing this is useful because we wish to consider the conditional coverage probability for a user located at a random distance from the macrocell DBS. Conditional coverage probability should be expanded to cover the whole space with the probability distribution function $f_{X_{j}|\text{in}}(x)$.

We define a random variable X_j as the distance between a typical user k and the BS in the tier j that provides service. Suppose the distance between the typical user and the nearest BS in the tier j is R_j; then the relationship between X_j and R_j can be written as

$$\mathbb{P}[X_j \le x] = \mathbb{P}[R_j \le x | u_k \overset{a.s.}{=} j]. \tag{12}$$

The conditional cumulative distribution function of X_j can be written as

$$F_{X_{j}|\text{in}}(x) = \mathbb{P}\left[X_j \le x | u_k \in C\right]$$
$$= \mathbb{P}\left[R_j \le x | u_k \overset{a.s.}{=} j, u_k \in C\right]. \tag{13}$$

The probability density function (PDF) of X_j can be calculated as follows:

$$f_{X_{j}|\text{in}}(x) = \frac{dF_{X_{j}|\text{in}}(x)}{dx}. \tag{14}$$

A detailed deviation of the PDF can be found in Appendix C and D, and the results are shown in Lemmas 3 and 4.

Lemma 3: The PDF of the distance between a typical user and the serving BS in the macrocell tier is

$$f_{X_{m}|\text{in}}(x) = \frac{dF_{X_{m}|\text{in}}(x)}{dx}$$
$$= \frac{2\pi\lambda_1}{A_{m|\text{in}}} * \exp\left\{-\lambda_d \pi (P_m^f K_m^f)^{\frac{2}{\alpha^f}} x^{\frac{2*\alpha^m}{\alpha^f}} - \pi\lambda_1 x^2\right\} x. \tag{15}$$

Proof: See Appendix C for details. ∎

Lemma 4: The PDF of the distance between a typical user and the serving BS in the femtocell tier is

$$f_{X_{f}|\text{in}}(x) = \frac{dF_{X_{f}|\text{in}}(x)}{dx}$$
$$= \frac{2\pi\lambda_d}{A_{f|\text{in}}} * \exp\left\{-\lambda_1 \pi (P_f^m K_f^m)^{\frac{2}{\alpha^m}} x^{\frac{2*\alpha^f}{\alpha^m}} - \pi\lambda_d x^2\right\} x \tag{16}$$

Proof: See Appendix D for details. ∎

V. CONDITIONAL COVERAGE PROBABILITY

In this section, we further analyze the conditional coverage probability. By coverage, we mean that a user may communicate smoothly, since the SINR is larger than a given threshold.

The conditional coverage probability is the probability of coverage given the deployment features of the macrocell and femtocell BSs, and given that the user is within a cluster. It is denoted as $c_{j|\text{in}}$, and can be written as follows:

$$c_{j|\text{in}} = A_{j|\text{in}} * c'_{j|\text{in}} \tag{17}$$

where j also equals m or f for different communication tier.

Prior to beginning service, the communication system should decide which tier is suitable for a given user, which is represented as $A_{j|\text{in}}$ and was discussed in Section IV.

Since macrocell and femtocell follow two different kinds of distribution in this study, it is hard to analyze one and copy to the other one. Then, we study both the cases as follows:

1) Case 1: The user is associating with macrocell.
2) Case 2: The user is associating with femtocell.

Furthermore, to be a comprehensive study, we consider the following two types of spectrum allocation strategies:

1) Type 1: There is no same tier interference, due to channel allocation algorithms in the adjacent cells. For example, in a cellular communication network, a group of frequencies can be reused in other cells, and the same frequencies are not reused in adjacent neighboring cells to avoid interference [37].

   Each BS serves a group of associated users in a time-division manner. Due to the broadcast feature of wireless signals, their data transmission causes interference at users associated with the other tier. For a typical user k served by a BS l in the tier j, the interference from tier $j-$ can be written as

$$I_k^j = I_{(k,j-)}^j = \sum_{l \in \Theta_{j-}} P^{j-} h_{\text{kl}}^{j-} g(d_{\text{kl}}). \tag{18}$$

2) Type 2: A general case that interference exists in both tiers, with the following representation:

$$I_k^j = I_{(k,f)}^j + I_{(k,m)}^j = \sum_{j \in (m,f)} \sum_{l \in \Theta_j \setminus B_k} P^j h_{\text{kl}}^j g(d_{\text{kl}}) f \tag{19}$$

where the interference I_k^j is from both macrocell $I_{(k,m)}^j$ and femtocell $I_{(k,f)}^j$. B_k is to represent the associated BS with the user k.

A. Case 1: The User is Associating With Macrocell

We first analyze conditional coverage probability when the typical user is associating with macrocell tier, i.e., $c_{m|\text{in}}$.

Due to (17), the conditional coverage probability is further represented as follows:

$$c_{m|\text{in}} = A_{m|\text{in}} * \mathbb{P}[\text{SINR(z)} > \tau | u_k \in C]$$
$$= A_{m|\text{in}} * \int_{R^2} \mathbb{P}[\text{SINR(z)} > \tau | u_k \in C] f_{X_{m}|\text{in}}(z) dz \tag{20}$$

where z is the location of DBS in macrocell tier, and where $f_{X_{m}|\text{in}}$ denotes the PDF of the distance in Lemma 3. C is used to represent a cluster/refuge.

Then the next step is to solve $\mathbb{P}[\text{SINR(z)} > \tau | u_k \in C]$ as follows (for simplicity, we denote this as $\mathbb{P}_z^m$); this relation

indicates that the SINR is larger than a given threshold if the user remains within a cluster:

$$
\mathbb{P}_z^m = \mathbb{P}[\text{SINR}(z) > \tau | u_k \in C]
$$

$$
\overset{(1)}{=} \mathbb{P}\left[h > \frac{[I_k^m + \sigma^2]\tau z^{a^m}}{K_m P^m} \right]_{u_k \in C}
$$

$$
\overset{(2)}{=} \exp\left(-\frac{[I_k^m + \sigma^2]\tau z^{a^m}}{K_m P^m} \right)_{u_k \in C}
$$

$$
= \exp\left(-\frac{\tau z^{a^m} \sigma^2}{K_m P^m} \right) \exp\left(-\frac{I_k^m \tau z^{a^m}}{K_m P^m} \right)_{u_k \in C} \quad (21)
$$

where step 1) is based on the definition of the SINR in (5), and step 2) is based on the assumption that the impact of Rayleigh fading follows as exponential distribution, as described in Section III-B.

Then, I_k^m in (21) will be expanded based on the two types of spectrum usage as follows.

1) Type 1: There is no Same Tier Interference: We first consider the type 1, so that $\mathbb{P}_z^m$ is further represented as follows, by only considering interference from femtocell BSs:

$$
\mathbb{P}_z^m = \exp\left(-\frac{\tau z^{a^m} \sigma^2}{K_m P^m} \right) \mathcal{L}_{I_{(k,f)}^m}\left(\frac{z^{a^m} \tau}{K_m P^m} \right)_{u_k \in C}. \quad (22)
$$

The basic procedures to solve it include:

1) expanding Laplace Transform $\mathcal{L}_{I_{(k,f)}^m}\left(\frac{z^{a^m}\tau}{K_m P^m}\right)_{u_k \in C}$ based on (18);

2) representing the distribution of femtocell BSs based on probability-generating function for PCP;

3) integrating steps 1) and 2) to solve $\mathcal{L}_{I_{(k,f)}^m}\left(\frac{z^{a^m}\tau}{K_m P^m}\right)_{u_k \in C}$.

The detailed deviation of $\mathcal{L}_{I_{(k,f)}^m}\left(\frac{z^{a^m}\tau}{K_m P^m}\right)_{u_k \in C}$ can be found in Appendix E. In step 3), some mathematic manipulation, e.g., approximation, is necessary for the inextricable problem. And finally we reach the approximate theoretical upper bound of conditional coverage probability in Theorem 1 .

Theorem 1: For a typical user, the approximate theoretical upper bound on the conditional coverage probability, denoted as $\widetilde{c}_{m|\text{in}}$, for the macrocell tier in type 1 is

$$
\widetilde{c}_{m|\text{in}} = 2\pi\lambda_1 \int_0^\infty z \exp\left\{ -\frac{\tau}{P^m K_m} z^{a^m} \sigma^2 - \pi\lambda_1 z^2 + \widetilde{\mathcal{K}}_f(.) \right.
$$

$$
\left. - \lambda_d \pi (P_m^f K_m^f)^{\frac{2}{a^f}} z^{\frac{2*\alpha^m}{\alpha^f}} \right\} dz \quad (23)
$$

where

$$
\widetilde{\mathcal{K}}_f(.) = -\frac{\mu * \lambda_c * 2\pi}{(\mu+1)} * \left\{ \frac{1}{B^{\frac{2}{a}}(a^f-2) * \min^{\frac{a^f-2}{a^f}}} \right.
$$

$$
* \cdot {_2F_1}\left(\frac{a^f-2}{a^f}, \frac{a^f-2}{a^f}; \frac{2a^f-2}{a^f}; \frac{1}{\min} \right)
$$

$$
- \frac{\frac{2D_c}{3}}{B^{\frac{1}{a}}(a^f-1) * \min^{\frac{a^f-1}{a^f}}}
$$

$$
\left. * \cdot {_2F_1}\left(\frac{a^f-1}{a^f}, \frac{a^f-1}{a^f}; \frac{2a^f-1}{a^f}; \frac{1}{\min} \right) \right\}
$$

$$
(24)
$$

and $B = [\tau z^{a^m} P_m^f \frac{K_f}{K_m}(\mu+1)]^{-1}$, $\min = B(\frac{2D_c}{3})^{a^f} + 1$.

Input of $\widetilde{\mathcal{K}}_f(.)$ includes BS power P^m and P^f, pass loss factors a^m, a^f, K_m, and K_f, radius of cluster D_c, the mean number of points in each cluster u, cluster density λ_c, and threshold τ.

2) Type 2: Interference Exists in Both Tiers: In type 2, the interference will be considered as shown in (19), so that $\mathbb{P}_z^m$ is further represented as follows:

$$
\mathbb{P}_z^m = \exp\left(-\frac{\tau z^{a^m} \sigma^2}{K_m P^m} \right) \mathcal{L}_{I_{(k,m)}^m}\left(\frac{z^{a^m}\tau}{K_m P^m} \right)_{u_k \in C} \mathcal{L}_{I_{(k,f)}^m}
$$

$$
\times \left(\frac{z^{a^m}\tau}{K_m P^m} \right)_{u_k \in C}. \quad (25)
$$

The basic procedures to solve $\mathcal{L}_{I_{(k,m)}^m}\left(\frac{z^{a^m}\tau}{K_m P^m}\right)_{u_k \in C}$ are similar to the deviations in Section V-A.1 and Appendix E.

First, Laplace Transform of $\mathcal{L}_{I_{(k,m)}^m}\left(\frac{z^{a^m}\tau}{K_m P^m}\right)_{u_k \in C}$ is expanded based on the interference expression in (19) as follows:

$$
\mathcal{L}_{I_{(k,m)}^m}\left(\frac{z^{a^m}\tau}{K_m P^m} \right) = \mathbb{E}_{h_m,\Theta_m}\left[\exp\left(-\frac{z^{a^m}\tau I_{(k,m)}^m}{K_m P^m} \right) \right]
$$

$$
= \mathbb{E}_{h_m,\Theta_m}\left[\exp\left(-\frac{z^{a^m}\tau}{K_m P^m} \sum_{l \in \Theta_m/B_k} P^m h_{kl}^m K_m d_{kl}^{-a^m} \right) \right]
$$

$$
\overset{(3)}{=} \mathbb{E}_{\Theta_m}\left[\prod_{l \in \Theta_m/B_k} \frac{1}{1 + s_3(d_{kl})^{-a^m}} \right] \quad (26)
$$

where $s_3 = \tau z^{a^m}$.

Step 3) follows from the moment-generating function [38] of an exponentially distributed random variable h^m, as follows:

$$
\mathbb{E}_h[e^{-sR}] = \frac{1}{1 + sR}. \quad (27)
$$

Second, since BSs in macrocell tier follow a PPP distribution, its probability-generating function [10] is as follows:

$$
G_P(v(x)) = \mathbb{E}\left[\prod v(x) \right] = \exp\left(-\lambda_1 \int_{R^2} (1 - v(x))dz \right). \quad (28)
$$

Third, by comparing (26) and (28), it is easy to find $v(x) = \frac{1}{1+s_3(d_{kl})^{-a^m}}$, and then integrating them together we have

$$
\mathcal{L}_{I_{(k,m)}^m}\left(\frac{z^{a^m}\tau}{K_m P^m} \right) = \exp\left(-\lambda_1 \int_{R^2}\left(1 - \frac{1}{1 + s_3 * z^{-a^m}} \right) dz \right)
$$

$$
\overset{(4)}{=} \exp\left(-\lambda_1(s_3)^{2/a^m} C(a^m) \right). \quad (29)
$$

Step 4) is adopted based on the analysis result, i.e., (17) in [39], where $C(a^m) = \frac{2\pi^2 C S(\frac{2\pi}{a^m})}{a^m}$

Finally, by substituting results of $\mathcal{L}_{I_{(k,m)}^m}\left(\frac{z^{a^m}\tau}{K_m P^m}\right)_{u_k \in C}$, $\mathcal{L}_{I_{(k,f)}^m}\left(\frac{z^{a^m}\tau}{K_m P^m}\right)_{u_k \in C}$, Lemmas 1 and 3 together we reach to Corollary 1 as follows.

Corollary 1: For a typical user, the approximate theoretical upper bound on the conditional coverage probability for the

macrocell tier in type 2, denoted as $\widetilde{c}_{m|\text{in}}$, is

$$\widetilde{c}_{m|\text{in}} = 2\pi\lambda_1 \int_0^\infty z \exp\left\{ -\frac{\tau}{P^m K_m} z^{a^m} \sigma^2 - \pi\lambda_1 z^2 + \widetilde{\mathcal{K}}_f(.) \right.$$
$$- \lambda_1 (s_3)^{2/a^m} C(a^m)$$
$$\left. - \lambda_d \pi (P_m^f K_m^f)^{\frac{2}{a^f}} x^{\frac{2*\alpha^m}{a^f}} \right\} dz \quad (30)$$

where $\widetilde{\mathcal{K}}_f(.)$ has the same form as in Theorem 1.

B. Case 2: The User is Associated With Femtocell

Then we further analyze the case that the typical user is associated with femtocell, which is denoted as $c_{f|\text{in}}$, and can be represented as follows,

$$c_{f|\text{in}} = A_{f|\text{in}} * \mathbb{P}[\text{SINR(z)} > \tau|u_k \in C]$$
$$= A_{f|\text{in}} * \int_{R^2} \mathbb{P}[\text{SINR(z)} > \tau|u_k \in C] f_{X_f|\text{in}}(z) dz \quad (31)$$

where z is the location of femtocell BS.

Then similarly to (21), we short $\mathbb{P}[\text{SINR(z)} > \tau|u_k \in C]$ in (31) as $\mathbb{P}_z^f$, and then further analyze it as follows:

$$\mathbb{P}_z^f = \mathbb{P}[\text{SINR(z)} > \tau|u_k \in C]$$
$$= \exp\left(-\frac{\tau z^{a^f} \sigma^2}{K_f P^f}\right) \exp\left(-\frac{I_k^f \tau z^{a^f}}{K_f P^f}\right)_{u_k \in C}. \quad (32)$$

I_k^f is expanded based on the following two types of spectrum allocation.

1) Type 1: There is no Same Tier Interference: In type 1, the interference will form macrocell BSs, for the user who is served by a femtocell BS. Then, $\mathbb{P}_z^f$ is further represented as follows from (32):

$$\mathbb{P}_z^f = \exp\left(-\frac{\tau z^{a^f} \sigma^2}{K_f P^f}\right) \mathcal{L}_{I_{(k,m)}^f}\left(\frac{z^{a^f} \tau}{K_f P^f}\right)_{u_k \in C}. \quad (33)$$

Then, the interference from macrocell BSs, i.e., $\mathcal{L}_{I_{(k,m)}^f}(\frac{z^{a^f}\tau}{K_f P^f})_{u_k \in C}$ is further expanded as follows:

$$\mathcal{L}_{I_{(k,m)}^f}\left(\frac{z^{a^f} \tau}{K_f P^f}\right)$$
$$= \mathbb{E}_{h_m,\Theta_m}\left[\exp\left(-\frac{z^{a^f} \tau I_{(k,m)}^f}{K_f P^f}\right)\right]$$
$$= \mathbb{E}_{h_m,\Theta_m}\left[\exp\left(-\frac{z^{a^f} \tau}{K_f P^f} \sum_{l \in \Theta_m/k} P^m h_{kl}^m K_m d_{kl}^{-a^m}\right)\right]$$
$$= \mathbb{E}_{\Theta_m}\left[\prod_{l \in \Theta_m/k} \frac{1}{1 + s_3^{(2)}(d_{kl})^{-a^m}}\right] \quad (34)$$

where $s_3^{(2)} = \tau z^{a^m} K_f^m P_f^m$, similar to the analysis process in (26).

Then, since the macrocell tier follows a PPP distribution, we have

$$\mathcal{L}_{I_{(k,m)}^f}\left(\frac{z^{a^f} \tau}{K_f P^f}\right) = \exp\left(-\lambda_1 \int_{R^2}\left(1 - \frac{1}{1 + s_3^{(2)} * z^{-a^m}}\right) dz\right)$$
$$= \exp\left(-\lambda_1 (s_3^{(2)})^{2/a^m} C(a^m)\right) \quad (35)$$

where $C(a^m) = \frac{2\pi^2 C S(\frac{2\pi}{a^m})}{a^m}$, similar to the analysis process in (29).

Finally, by substituting the results in (35), (33), Lemma 2, and Lemma 4 into (31), we reach to the Theorem 2 as follows.

Theorem 2 For a typical user, the approximate theoretical upper bound on the conditional coverage probability, denoted as $\widetilde{c}_{f|\text{in}}$, for the femtocell tier with a Matern cluster process in type 1 is

$$\widetilde{c}_{f|\text{in}} = 2\pi\lambda_d \int_0^\infty z \exp\left\{ -\frac{\tau}{P^f K_f} z^{a^f} \sigma^2 - \pi\lambda_d z^2 \right.$$
$$- \lambda_1 (s_3^{(2)})^{2/a^m} C(a^m)$$
$$\left. - \lambda_1 \pi (P_f^m K_f^m)^{\frac{2}{a^f}} x^{\frac{2*\alpha^m}{a^f}} \right\} dz \quad (36)$$

2) Type 2: Interference Exists in Both Tiers: Considering the type that interference exists in both tiers, we have

$$\mathbb{P}_z^f = \mathbb{P}[\text{SINR(z)} > \tau|u_k \in C]$$
$$= \exp\left(-\frac{\tau z^{a^f} \sigma^2}{K_f P^f}\right) \mathcal{L}_{I_{(k,m)}^f}\left(\frac{z^{a^f} \tau}{K_f P^f}\right)_{u_k \in C} \mathcal{L}_{I_{(k,f)}^f}$$
$$\times \left(\frac{z^{a^f} \tau}{K_f P^f}\right)_{u_k \in C} \quad (37)$$

Then take the similar process in Appendix E, $\mathcal{L}_{I_{(k,f)}^f}(\frac{z^{a^f}\tau}{K_f P^f})$ can be solved by first expanding the Laplace transform

$$\mathcal{L}_{I_{(k,f)}^f}\left(\frac{z^{a^f} \tau}{K_f P^f}\right) = \mathbb{E}_{\Theta_f}\left[\prod_{i \in \Theta_f} \frac{1}{1 + s_2^{(2)}(d_i)^{-a^f}}\right] \quad (38)$$

where $s_2^{(2)} = \tau z^{a^f}$.

And second solve $\mathcal{L}_{I_{(k,f)}^f}(\frac{z^{a^f}\tau}{K_f P^f})$ based on probability-generating function for PCP similar to Appendix E.

Then, the upper bound is calculated as follows:

$$\widetilde{\mathcal{K}}_f^{(2)}(.) = -\frac{\mu * \lambda_c * 2\pi}{(\mu + 1)}$$
$$* \left\{ \frac{1}{(B^{(2)})^{\frac{2}{a}}(a^f - 2) * (\min^{(2)})^{\frac{a^f - 2}{a^f}}} \right.$$
$$* \, _2F_1\left(\frac{a^f - 2}{a^f}, \frac{a^f - 2}{a^f}; \frac{2a^f - 2}{a^f}; \frac{1}{\min^{(2)}}\right)$$
$$- \frac{\frac{2D_c}{3}}{(B^{(2)})^{\frac{1}{a}}(a^f - 1) * (\min^{(2)})^{\frac{a^f - 1}{a^f}}}$$
$$\left. * \, _2F_1\left(\frac{a^f - 1}{a^f}, \frac{a^f - 1}{a^f}; \frac{2a^f - 1}{a^f}; \frac{1}{\min^{(2)}}\right) \right\}$$
$$\quad (39)$$

where $B^2 = [s_2^{(2)}(\mu + 1)]^{-1}$, and $\min^{(2)} = B^{(2)}(\frac{2D_c}{3})^{a^f} + 1$.

Finally, by substituting results in (35) and (39) into (31), we get to the **Corollary 2** as follows.

Corollary 2: For a typical user, the approximate theoretical upper bound on the conditional coverage probability, denoted as $\widetilde{c}'_{f|\text{in}}$, for the femtocell tier with a Matern cluster process in type 2 is

$$\widetilde{c}'_{f|\text{in}} = 2\pi\lambda_d \int_0^\infty z \exp\left\{ -\frac{\tau}{P^f K_f} z^{a^f} \sigma^2 - \pi\lambda_d z^2 + \widetilde{\mathcal{K}}_f^{(2)}(.) \right.$$
$$- \lambda_1 (s_3^{(2)})^{2/a^m} C(a^m)$$
$$\left. - \lambda_1 \pi (P_f^m h_f^m K_f^m)^{\frac{2}{\alpha^f}} x^{\frac{2*\alpha^m}{\alpha^f}} \right\} dz. \quad (40)$$

VI. SOLVING DMP

Through the mathematic analysis results in Sections IV and V, DMP can be rewritten approximately as

DMP: min λ_1 subject to:

$$\widetilde{c}_{m|\text{in}} \geq \eta_1, \quad (41)$$
$$\widetilde{c}_{f|\text{in}} \geq \eta_2, \quad (42)$$
$$P^m \geq P^f, \quad 0 < \lambda_1 < 1, \quad 0 < \lambda_d < 1 \quad (43)$$

where

$$\widetilde{c}_{m|\text{in}} = 2\pi\lambda_1 \int_0^\infty z \exp\left\{ -\frac{\tau}{P^m} z^{a^m} \sigma^2 - \pi\lambda_1 z^2 + \widetilde{\mathcal{K}}_f(.) \right.$$
$$\left. - \lambda_d \pi (P_m^f K_m^f)^{\frac{2}{\alpha^f}} z^{\frac{2*\alpha^m}{\alpha^f}} \right\} dz \quad (44)$$

and

$$\widetilde{c}_{f|\text{in}} = 2\pi\lambda_d \int_0^\infty z \exp\left\{ -\frac{\tau}{P^f K_f} z^{a^f} \sigma^2 - \pi\lambda_d z^2 \right.$$
$$- \lambda_1 (s_3')^{2/a^m} C(a^m) \quad (45)$$
$$\left. - \lambda_1 \pi (P_f^m K_f^m)^{\frac{2}{\alpha^f}} x^{\frac{2*\alpha^m}{\alpha^f}} \right\} dz.$$

Here we take the results in Theorems 1 and 2 as constraints to solve DMP. The results in Corollaries 1 and 2 can be adopted in a similar way based on different application requirement.

Unfortunately, the above problem is intractable because there is no closed-form expression of (44) and (45). To address this challenge, we propose to approximate (44) and (45) using linear constraints. Specifically, we consider a linear expression $\phi\lambda_1^2 + \psi\lambda_1 + \omega$ to replace the integration term in (44) and (45), where ϕ, ψ, and ω are parameters needed to be determined according to numerical values of (31). By using the fitting function provided by MATLAB, we can easily get ϕ, ψ, and ω.

For this purpose, we approximate the integral part with numerical fitting. The corresponding constraints can be rewritten as

$$\widetilde{c}_{m|\text{in}} = -4.38\lambda_1^2 + 2.78\lambda_1 + 0.4 \quad (46)$$
$$\widetilde{c}_{f|\text{in}} = 4.34\lambda_1^2 - 2.87\lambda_1 + 0.68 \quad (47)$$

TABLE I
ERROR BETWEEN TWO EQUATIONS (44) AND (46)

	1	2	3	4	5	6	7
error	−0.03	0.005	0.019	0.02	0.015	0.007	−0.001
	8	9	10	11	12	13	14
error	−0.008	−0.013	−0.014	−0.012	0.006	0.004	0.018

when $P^m = 40$ dBm, $P^f = 33$ dBm, $a^m = 3$, $a^f = 3$, $\lambda_d = \frac{10}{\pi(500\,\text{m})^2}$, $\lambda_c = \frac{20}{\pi(5\,\text{km})^2}$, and $\tau = 5$.

Errors between two equations (44) and (46) are shown in Table I, which represents the acceptable accuracy of approximate expression by using numerical fitting. The original problem can be approximated by a problem with linear constraints (46) and (47), which can be easily solved by using existing mathematical tools, such as CPLEX. Similar sutdy has been done between (45) and (47) with similar small errors.

VII. EVALUATION

We used MATLAB to perform a numerical evaluation of the accuracy of our analysis and performance of the optimization.

A. Accuracy of the Coverage Probability Study

To determine the accuracy of our analysis, we performed the following evaluations. First, to evaluate the accuracy of the conditional coverage probability (Theorem 1), we compared our results to those of a simulated network environment, in which were deployed DBSs in macrocell tier following a homogeneous PPP distribution and femtocell BSs following a PCP distribution; the area was a square of side length 10 km. An image of the simulation can be seen in Fig. 5, where triangles indicate the macrocell DBSs, blue dots indicate the femtocell BSs, and yellow crosses indicate the centers of the clusters. The densities were preliminarily set as follows: macrocell DBSs, $\lambda_1 = \frac{3}{\pi(5\,\text{km})^2}$; clusters, $\lambda_c = \frac{20}{\pi(5\,\text{km})^2}$; femtocell BSs, $\lambda_d = \frac{10}{\pi(500\,\text{m})^2}$; and $K_m = 100K_f$ to indicate influence from obstacles in refuge.

We randomly selected a user in a cluster, measured the corresponding SINR, and calculated the coverage probability. This was a Monte Carlo simulation, and the results were used to evaluate the accuracy of our analysis.

More specifically, in the simulation, femtocell BSs were generated following PCP distribution 1000 times based on the definition of Matern cluster process [10], [40] as described in Section III-A. In each generation, a user within a cluster was randomly selected, and then association relation was judged based on the received power from macrocell and femtocell BSs. After that, SNIR value was measured based on the distance between the user and the associated BS. Finally, whether the user can receive an acceptable communication service was estimated based on SNIR. After 1000 times generations, the conditional association/coverage possibilities were measured and seen as a criterion to evaluate the analysis results in this study.
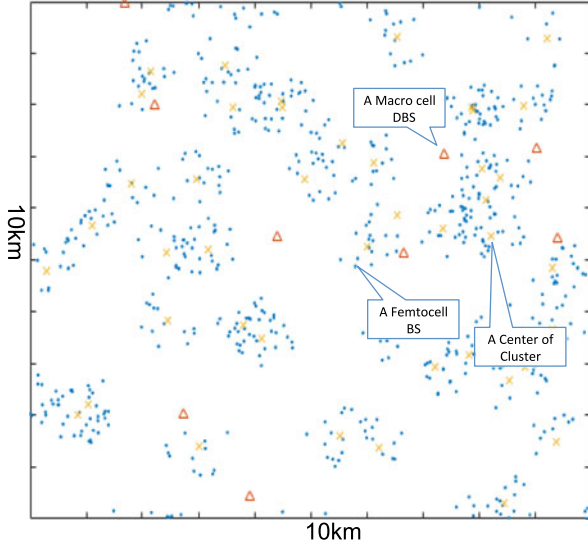
Fig. 5. Simulation environment.

Meanwhile, a lot of tests have been done to find the confidence interval in Monte Carlo simulation, and finally a smooth and stable result could be reached at 1000.

Fig. 6(a) shows the evaluation results for various levels of power (P^m) in the macrocell DBSs, and for various settings of the interference threshold τ. The values of $C_{\text{Analysis}}^{\text{in}}$ indicated by open circles are the results based on Theorem 1, and the lines indicate the results based on the Monte Carlo simulation. Symbols and lines are used similarly in Fig. 6.

From Fig. 6(a), we can see that the analysis is acceptably accurate, since the results match those of the simulation for various values of P^m and τ. However, we have observed the following: 1) the coverage probability of the macrocells is not low, even when the user is inside of a cluster of femtocell BSs and 2) the coverage probability may decrease when the macrocell DBSs have a lower power output P^m. In such a situation, deployment of femtocell BSs to shelters can be expected to increase communication services.

We have evaluated the accuracy of Lemma 1, the conditional association probability, for a user within a cluster of femtocell BSs. Fig. 6(b) shows the accuracy of our analysis. We have observed the following two phenomena: 1) with the setting parameters in the simulation, the conditional association probability is rather high; and 2) the conditional association probability does not appear to be affected by the communication threshold τ.

B. Performance Evaluation

In this section, we evaluate our estimate of the coverage probability. We consider the following two scenarios, in which small-cell BSs are used to enhance communication.

1) Scenario 1 (S1): The macrocell DBSs work well with enough power (e.g., $P^m = 50$ dBm). In this case, the communication resources will be insufficient at locations where there are crowds of people, especially when users are transferring videos, e.g., at refuges. We assume that

low power femtocell BSs (i.e., $P^f = 23$ dBm) are deployed around the location in order to enhance communication.

2) Scenario 2 (S2): The macrocell DBSs work with shortage power, e.g., the transmission power may be as low as 10 W ($P^m = 40$ dBm). To enhance communication, more powerful (2 W) femtocell BSs are deployed ($P^f = 33$ dBm) in refuges.

As in Section VII-A, we used a Monte Carlo simulation to evaluate the accuracy with various density of femtocell and macrocell DBSs.

First, we evaluated the performance of the conditional coverage probability for various density of femtocell BSs, i.e., λ_d.

Fig. 6(c) shows the evaluation results for various values of the density (λ_d) of the femtocell BSs for both scenarios S1 and S2. From Fig. 6(c), we can see that the analysis results match those of the simulation. We observe the following: 1) the coverage probability decreases with an increased density of the femtocell BSs; and 2) the performance of the macrocell DBSs is poor when the density of the femtocell BSs is too large.

Therefore, as with the results in Fig. 6(c), we clearly see the importance of the femtocell BSs in the disaster scenario, since otherwise, the conditional coverage probability is rather poor. Furthermore, we note that when the density of the femtocell BSs is increased, their importance to scenario S1 becomes clear, since the conditional coverage probability becomes poor.

We further evaluated the performance of the conditional coverage probability for various density of macrocell λ_1, respectively.

Fig. 6(d) shows the results for various macrocell densities, for both scenarios S1 and S2. In Fig. 6(d), we can see that, for various values of the macrocell density, our results match those of the simulation. We observe the following: 1) the coverage probability increases with the increased density of the macrocell DBSs; and 2) considering the wide deployment of macrocell DBSs (fewer than four macrocell DBSs in a 5 km square area), the performance is rather poor, and it does not provide sufficient communication services in a disaster scenario. Therefore, understanding minimal required number of macrocell DBSs is rather important, as studied in Section III-C.

Meanwhile, we have evaluated the cases with different value of pass loss factors K_m and K_f. In Fig. 6, K_m is set as 100 times of K_f to indicate the attenuation from obstacles in a refuge. Here, K_m is further set equal to K_f, to simulate a wide open space environment. The result is shown in Fig. 7. Comparing with Fig. 6(a), the conditional coverage probability in Fig. 7 becomes smaller when there is no obstacle attenuation, due to the stronger interference from femtocell BSs in a wide open space environment.

C. Optimization Evaluation

And finally we evaluated the optimization result of DMP studied in Section VI and the results are shown in Fig. 8.

Three cases were studied in the evaluation, i.e., case 1: $C_m > 0.55, C_f > 0.2$, case 2: $C_m > 0.35, C_f > 0.35$, and case 3: $C_m > 0.2, C_f > 0.55$. In each case, the density of macrocell
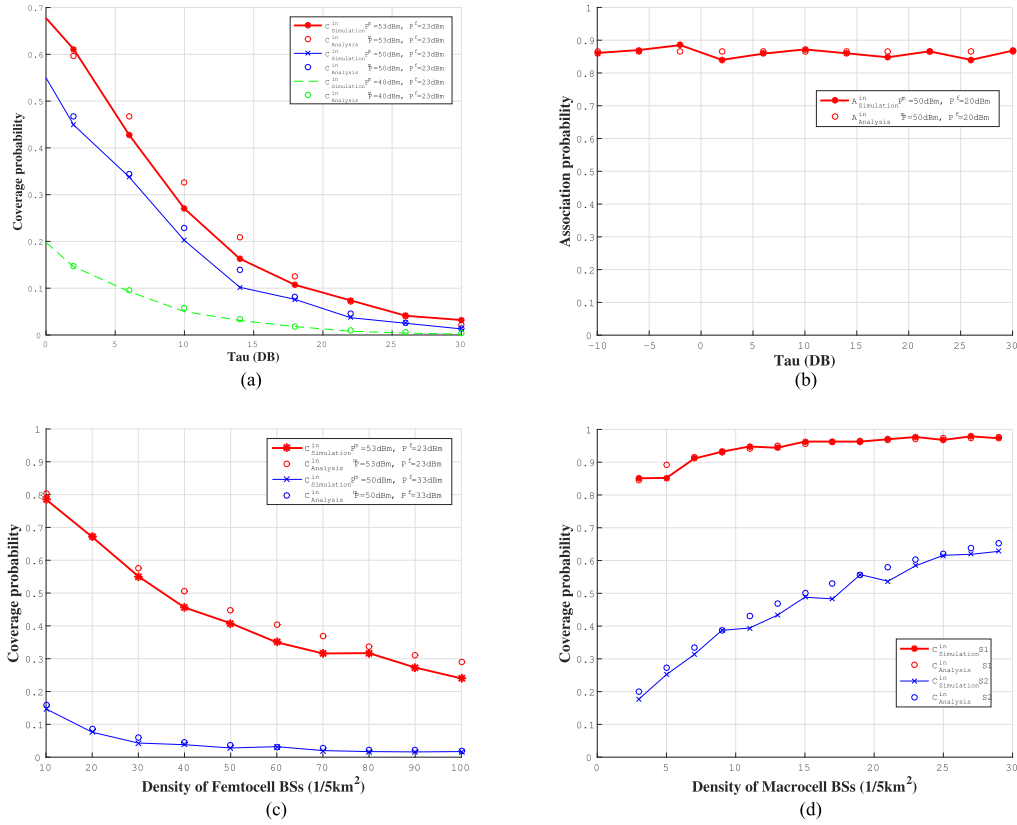
Fig. 6. Simulation results. (a) Coverage probability evaluation with settings τ from 0 to 30 dB, $\lambda_1 = \frac{3}{\pi (5\text{km})^2}$, $\lambda_d = \frac{10}{\pi (500\text{m})^2}$, and $\lambda_c = \frac{20}{\pi (5\text{km})^2}$. (b) Associate probability evaluation with settings τ from 0 to 30 dB, $\lambda_1 = \frac{3}{\pi (5\text{km})^2}$, $\lambda_d = \frac{10}{\pi (500\text{m})^2}$, and $\lambda_c = \frac{20}{\pi (5\text{km})^2}$. (c) Coverage probability evaluation with settings λ_d from $\frac{10}{\pi (500\,\text{m})^2}$ to $\frac{100}{\pi (500\,\text{m})^2}$, $\tau = 5$, $\lambda_1 = \frac{3}{\pi (5\,\text{km})^2}$, and $\lambda_c = \frac{20}{\pi (5\,\text{km})^2}$. (d) Coverage probability evaluation with settings λ_1 from $\frac{3}{\pi (5\,\text{km})^2}$ to $\frac{30}{\pi (5\,\text{km})^2}$, $\tau = 5$, $\lambda_d = \frac{10}{\pi (500\,\text{m})^2}$, and $\lambda_c = \frac{20}{\pi (5\,\text{km})^2}$.
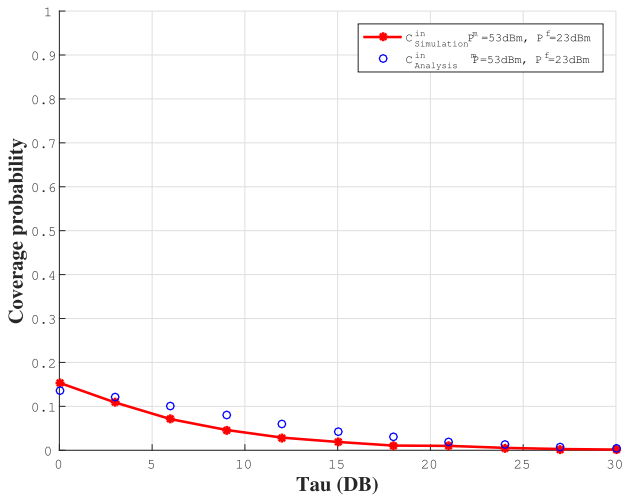

Fig. 7. Evaluation result of Theorem 1, with settings τ from 0 to 20 dB, $\lambda_1 = \frac{3}{\pi (5\,\text{km})^2}$, $\lambda_d = \frac{10}{\pi (500\,\text{m})^2}$, $\lambda_c = \frac{20}{\pi (5\,\text{km})^2}$, and $K_f = K_m$.

Fig. 8. Optimization results.

was increased gradually, and when C_m and C_f were both satisfied, the corresponding density was recorded. For a specific value of macrocell density, Monte Carlo simulation was also adopted to calculate conditional coverage probability. Similar to Section VII-A, femtocell and macrocell BSs were generated
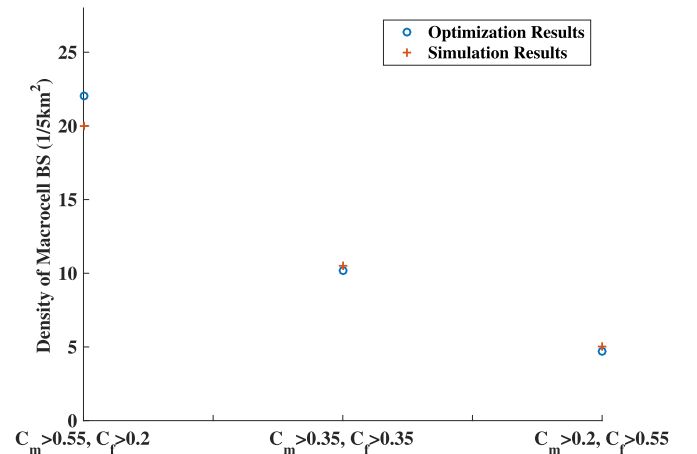
1000 times, and a user in cluster was randomly, and finally conditional coverage probabilities were calculated. For each case, we performed the above processes for 20 times, and the average value of macrocell density were used to be criterions, which are marked as red cross in Fig. 8, to evaluate the results from this study, marked as blue circle in Fig. 8. From the evaluation results

we can find the proposed method works well to final minimal density of macrocell BS, while guaranteeing the constraints.

VIII. CONCLUSION

In this paper, we analyzed the conditional association probability and the conditional coverage probability, for a small-cell communication network distributed according to a PCP and for a user remaining within a cluster. We defined an optimization problem to minimize the density of macrocell DBSs, while keeping acceptable coverage probability. We gave a clear definition of the probability and presented a detailed mathematic derivation, and solved the optimization problem. In addition, we evaluated our analysis by comparing our results to those of a Monte Carlo simulation of realistic scenarios. We evaluated the accuracy of our results. By performing this study, we determined that the deployment of femtocell BSs is useful for improving communications for crowds of people. We also determined that understanding minimal number of macrocell DBSs is rather important to keep QoE through the simulation. Finally, we determined and evaluated the minimal number of macrocell DBSs. In the future, we will study how to efficiently balance the communication resources of the two tiers.

APPENDIX A
PROOF OF LEMMA 1

In this section, we present the detailed derivation of $A_{m|\text{in}}$.

$$
\begin{aligned}
A_{m|\text{in}} &= \mathbb{P}\left[u_k \overset{a.s.}{=} m | u_k \in C\right] \\
&= \mathbb{P}\left[P_k^m > P_k^f | u_k \in C\right] \\
&\overset{(a)}{=} \mathbb{P}\left[R_m < (P_f^m K_f^m)^{\frac{1}{\alpha^m}} (R_f)^{\frac{\alpha^f}{\alpha^m}} | R_f \le D_0\right] \\
&\overset{(b)}{=} \int_0^{D_0} (1 - \exp\left\{-\pi\lambda_1 (P_f^m K_f^m)^{\frac{1}{\alpha^m}} r^{\frac{2\alpha^f}{\alpha^m}}\right\} * f_{R_f}(r) dr
\end{aligned}
$$
(48)

where R^m and R^f represent the distance from the nearest BS in macrocell and femtocell tiers, respectively. a^m and a^f are pass loss factors for macrocell and femtocell denoted in Section III-B. D_0 is the maximum range of R_f and it is calculated as follows in step (b).

First, the number of femtocell BSs in a cluster, denoted as n, can be calculated as $\pi D_c^2 \lambda_d$, since the density is λ_d, and the radius of the cluster is denoted as D_c. And we denote the coverage area of a femtocell BS as A_0, where $A_0 = \pi D_0^2$.

Then, the total area of the cluster, denoted as A, can be calculated as follows:

$$
A = \pi D_c^2 \overset{(c)}{\approx} n * A_0 = \pi D_c^2 \lambda_d * \pi D_0^2
$$
(49)

where Step (c) is based on the uniform distribution of femtocell BSs in a cluster.

By solving (49), we obtain the following:

$$
D_0 = \left(\frac{1}{\pi \lambda_d}\right)^{\frac{1}{2}}.
$$
(50)

In step (a), $\mathbb{P}[R_m < (P_f^m K_f^m)^{\frac{1}{\alpha^m}} (R_f)^{\frac{\alpha^f}{\alpha^m}}]$ can be solved using the distance function for a homogeneous PPP [41]

$$
\mathbb{P}[R \le r] = 1 - \exp\{-\pi\lambda r^2\}.
$$
(51)

$f_{R_f}(r)$ can also be calculated by using the same distance function [41]

$$
f_{R_f}(r) = \frac{d}{dr}\mathbb{P}[r_f \le r] = \exp(-\pi\lambda_d r^2) 2\pi\lambda_d r.
$$
(52)

Finally, we obtain

$$
\begin{aligned}
A_{m|\text{in}} = 2\pi\lambda_d \int_0^{D_0} &r \exp(-\pi\lambda_d r^2) \\
&* (1 - \exp\left\{-\pi\lambda_1 (P_f^m K_f^m)^{\frac{1}{\alpha^m}} r^{\frac{2\alpha^f}{\alpha^m}}\right\}) dr.
\end{aligned}
$$

The above calculation of D_0 is based on an assumption that each femtocell in one cluster does not overlap with other cells in the same cluster. Otherwise, the total areas covered by femtocell BSs will be larger than A as follows:

$$
A = \pi D_c^2 \overset{(c')}{\le} n * A_0 = \pi D_c^2 \lambda_d * \pi D_0^2.
$$
(53)

The above problem can be solved if the overlapped area can be detected, denoted as A_e, as follows, with an assumption that there is only the case that two femtocell BSs are overlapped:

$$
\pi D_c^2 + A_e = \pi D_c^2 \lambda_d * \pi D_0^2.
$$
(54)

APPENDIX B
PROOF OF LEMMA 2

The derivation for $A_{f|\text{in}}$ is similar to the process in Appendix A, as follows:

$$
\begin{aligned}
A_{f|\text{in}} &= \mathbb{P}\left[u_k \overset{a.s.}{=} f | u_k \in C\right] \\
&= \mathbb{P}\left[R_m > (P_f^m K_f^m)^{\frac{1}{\alpha^m}} (R_f)^{\frac{\alpha^f}{\alpha^m}} | R_f \le D_0\right] \\
&= \int_0^{D_0} \exp\left\{-\pi\lambda_1 (P_f^m K_f^m)^{\frac{1}{\alpha^m}} r^{\frac{2\alpha^f}{\alpha^m}}\right\} * f_{R_f}(r) dr.
\end{aligned}
$$
(55)

And finally, we have

$$
\begin{aligned}
A_{f|\text{in}} = 2\pi\lambda_d \int_0^{D_0} &r \exp(-\pi\lambda_d r^2) \\
&* \exp\left\{-\pi\lambda_1 (P_f^m K_f^m)^{\frac{1}{\alpha^m}} r^{\frac{2\alpha^f}{\alpha^m}}\right\} dr.
\end{aligned}
$$
(56)

APPENDIX C
PROOF OF LEMMA 3

In this section, we present the detailed derivation of the PDF $f_{X_m|\text{in}}(x)$. We consider a scenario such that the typical user is

associated with the macrocell layer:

$$F_{X_m \,|\mathrm{in}}(x) = \mathbb{P}[X_m > x | u_k \in C]$$

$$= \mathbb{P}[R_m \le x | k \overset{as.}{=} m, u_k \in C]$$

$$\overset{(d)}{=} \frac{\mathbb{P}[R_m \le x, k \overset{as.}{=} m | u_k \in C]}{A_{m|\mathrm{in}}}. \quad (57)$$

Step (d) is based on Bayes' theorem. For simplicity, we use the following notation: $\mathbb{P}_{m|\mathrm{in}}(x) = \mathbb{P}[R_m \le x, k \overset{as.}{=} m | u_k \in C]$.

$$\mathbb{P}_{m|\mathrm{in}}(x) = \mathbb{P}\left[R_m \le x, P_k^m > P_k^{f_i} | u_k \in C\right]$$

$$* f_{R_m \,|u_k \in C}(r)dr$$

$$\overset{(e)}{=} 2\pi\lambda_1 \int_0^x \left(\exp\left\{ -\lambda_d \pi (P_m^f K_m^f)^{\frac{2}{\alpha^f}} r^{\frac{2*\alpha^m}{\alpha^f}} \right\}\right.$$

$$\left. - \pi\lambda_1 r^2 \right\} r dr. \quad (58)$$

Step (e) is based on the distance function in (51), which is similar to Step (b) in the proof of Lemma 1, and $f_{R_m \,|u_k \in C}(r) = \exp(-\pi\lambda_1 r^2)2\pi\lambda_1 r$.

Thus, we have

$$f_{X_m \,|\mathrm{in}}(x) = \frac{dF_{X_m \,|\mathrm{in}}(x)}{dx}$$

$$= \frac{2\pi\lambda_1}{A_{m|\mathrm{in}}} * \exp\left\{-\lambda_d \pi (P_m^f K_m^f)^{\frac{2}{\alpha^f}} x^{\frac{2*\alpha^m}{\alpha^f}} - \pi\lambda_1 x^2\right\} x. \quad (59)$$

APPENDIX D
PROOF OF LEMMA 4

Derivation of the PDF $f_{X_f \,|\mathrm{in}}(x)$ is quite similar to the process in Appendix C.

Similar to (57)

$$F_{X_f \,|\mathrm{in}}(x) = \frac{\mathbb{P}[R_f \le x, k \overset{as.}{=} f | u_k \in C]}{A_{f|\mathrm{in}}}. \quad (60)$$

Finally, we get the result as follows:

$$f_{X_f \,|\mathrm{in}}(x) = \frac{dF_{X_f \,|\mathrm{in}}(x)}{dx}$$

$$= \frac{2\pi\lambda_d}{A_{f|\mathrm{in}}} * \exp\left\{-\lambda_1 \pi (P_f^m K_f^m)^{\frac{2}{\alpha^m}} x^{\frac{2*\alpha^f}{\alpha^m}} - \pi\lambda_d x^2\right\} x. \quad (61)$$

APPENDIX E
PROOF OF THEOREM 1

Here we present the detailed deviation to achieve Theorem 1. First since the interference is from the entire planet, we assume that $\mathcal{L}_{I_{(k,f)}^f}(\frac{z^{a^m}\tau}{K_m P^m})_{u_k \in C} \approx \mathcal{L}_{I_{(k,f)}^f}(\frac{z^{a^m}\tau}{K_m P^m})$.

Then, we take the following procedures in the deviation.

Procedure 1: Expanding $\mathcal{L}_{I_{(k,f)}^m}(\frac{z^{a^m}\tau}{K_m P^m})_{u_k \in C}$ based on interference expression in (18).

Since the interference $I_{(k,f)}^m$ depends on the position of the femtocell BSs in Θ_f and the parameter h_f, we have

$$\mathcal{L}_{I_{(k,f)}^m}\left(\frac{z^{a^m}\tau}{K_m P^m}\right)$$

$$= \mathbb{E}_{h_f, \Theta_f}\left[\exp\left(-\frac{z^{a^m}\tau I_{(k,f)}^m}{K_m P^m}\right)\right]$$

$$= \mathbb{E}_{h_f, \Theta_f}\left[\exp\left(-\frac{z^{a^m}\tau}{K_m P^m}\sum_{l \in \Theta_f} P^f h_{\mathrm{kl}}^f K_f d_{\mathrm{kl}}^{-a^f}\right)\right]$$

$$\overset{(f)}{=} \mathbb{E}_{\Theta_f}\left[\prod_{i \in \Theta_f} \frac{1}{1 + s_2(d_{\mathrm{kl}})^{-a^f}}\right] \quad (62)$$

where $s_2 = \tau z^{a^m} P_m^f \frac{K_f}{K_m}$.

Step (f) follows from the moment-generating function [38] of an exponentially distributed random variable h^f, as follows:

$$\mathbb{E}_h[e^{-sR}] = \frac{1}{1 + sR} \quad (63)$$

Procedure 2: Representing the distribution of femtocell BSs based on probability-generating function for PCP.

Since Θ^f follows a Matern cluster process, its probability-generating function can be described as shown in (64) through [10], [40]. We note that a probability-generating function is a useful tool for dealing with discrete random variables, since it transforms a sum into a product, and thus enables it to be handled more easily.

$$G_N(v(x))$$

$$= \mathbb{E}\left[\prod v(x)\right]$$

$$= \exp\left(-\lambda_c \int_{R^2}\left[1 - G_s\left(\overbrace{\int_{R^2} v(x+y)f(y)dy}^{f_{\mathrm{xy}}}\right)\right]dx\right)$$

$$\underbrace{\qquad\qquad\qquad\qquad}_{\mathcal{K}_f(.)}$$
$$(64)$$

where $G_s(f_{\mathrm{xy}}) = \exp(-\mu(1 - f_{\mathrm{xy}}))$ and μ is the mean number of daughter points in each cluster.

Procedure 3: Integrating the results in Procedures 1 and 2.

By comparing (62) and (64), it is clear that, in this case, $v(x)$ in the probability-generating function should be equal to $\frac{1}{1 + s_2(d_{\mathrm{kl}})^{-a^f}}$.

Then the interference from the femtocell, as shown in (62), can be calculated by substituting $\frac{1}{1 + s_2(d_{\mathrm{kl}})^{-a^f}}$ into (64)

as follows:

$$f_{xy} = \int_{R^2} v(x+y) f(y) dy$$

$$= \int_{R^2} \frac{1}{1 + s_2 ||x+y||^{-a^f}} f(y) dy \qquad (65)$$

where the distance between the user and the femtocell BS l, i.e., $d_k l$ in (62), is $||x+y||$, as shown in Section III-B, x is the location of the center of the cluster, and y is the location of the femtocell taking x as the origin.

Substituting the result of (65) to (64), and solving the integral in (64) can get the final result of $\mathcal{L}_{I_{(k,f)}^m} \left(\frac{z^{a^m} \tau}{K_m P^m} \right)$.

Then, we present the detailed mathematic manipulations in Procedure 4 as follows.

Procedure 4: Mathematic manipulations to solve (65) and (64)

First, the result of f_{xy} is shown below, and the mathematical details of Step (g) can be found in Appendix F.

$$f_{xy} \stackrel{(g)}{\le} \frac{1}{1 + s_2 \left(\left[\frac{2D_c}{3} + x \right] \right)^{-a^f}} \qquad (66)$$

Furthermore, based on the relation $\exp(-\delta x) \le \frac{1}{1+\delta x}$, (64) can be further simplified as follows:

$$G_N(v(x)) = \exp \left(-\lambda_c \int_{R^2} \{ 1 - \exp[-\mu(1-f_{xy})] \} dx \right)$$

$$\le \exp \left\{ -\lambda_c \int_{R^2} \left[1 - \frac{1}{1 + \mu(1-f_{xy})} \right] dx \right\}$$

$$= \exp \left\{ \underbrace{-\lambda_c \int_{R^2} \left[\frac{\mu(1-f_{xy})}{1 + \mu(1-f_{xy})} \right] dx}_{\mathcal{K}_f(.)} \right\}. \qquad (67)$$

By substituting the results for f_{xy} in (66) into $\mathcal{K}_f(.)$ of (67), we obtain $\mathcal{K}_f(.)$ as follows:

$$\mathcal{K}_f(.) \le \widetilde{\mathcal{K}}_f(.)$$

$$\stackrel{(h)}{=} -\frac{\mu * \lambda_c * 2\pi}{\mu + 1} \left\{ \int_{\frac{2D_c}{3}}^{\infty} \frac{t}{Bt^{a^f}+1} dt - \int_{\frac{2D_c}{3}}^{\infty} \frac{\frac{2D_c}{3}}{Bt^{a^f}+1} dt \right\}$$

$$= -\frac{\mu * \lambda_c * 2\pi}{(\mu+1)} * \left\{ \frac{1}{B^{\frac{2}{a}}(a^f-2) * \min^{\frac{a^f-2}{a^f}}} \right.$$

$$* \cdot_2F_1 \left(\frac{a^f-2}{a^f}, \frac{a^f-2}{a^f}; \frac{2a^f-2}{a^f}; \frac{1}{\min} \right)$$

$$- \frac{\frac{2D_c}{3}}{B^{\frac{1}{a}}(a^f-1) * \min^{\frac{a^f-1}{a^f}}}$$

$$\left. * \cdot_2F_1 \left(\frac{a^f-1}{a^f}, \frac{a^f-1}{a^f}; \frac{2a^f-1}{a^f}; \frac{1}{\min} \right) \right\} \qquad (68)$$

where $B = [s_2(\mu+1)]^{-1}$, and $\min = B(\frac{2D_c}{3})^{a^f} + 1$.

The mathematical details of Step (h) can be found in Appendix G.

Then, we obtain an upper bound on (64) as follows:

$$\widetilde{G}_N(v(x)) = \exp(\widetilde{\mathcal{K}}_f(.)). \qquad (69)$$

Since (62) and (64) have the same form, and we substitute the result of (62), i.e., $\frac{1}{1 + s_2(d_{k1})^{-a^f}}$, into (64) as a $v(x)$, $\exp(\widetilde{\mathcal{K}}_f(.))$ is also the upper bound of (62); this is denoted as $\widetilde{\mathcal{L}}_{I_{(k,f)}^f} \left(\frac{z^{a^m} \tau}{P^m} \right)$, and it can be written as follows:

$$\widetilde{\mathcal{L}}_{I_{(k,f)}^f} \left(\frac{z^{a^m} \tau}{P^m} \right) = \exp(\widetilde{\mathcal{K}}_f(.)). \qquad (70)$$

By substituting the results of (70) into (22), and integrating the results from Lemmas 1 and 3 into (20), we reach an upper bound of conditional coverage probability, denoted as $\widetilde{c}_{m|\text{in}}$ in Theorem 1 as follows:

$$\widetilde{c}_{m|\text{in}} = A_{m|\text{in}} * \int_{R^2} \widetilde{\mathbb{P}}[\text{SINR}(z) > \tau | u_k \in C] f_{X_m|\text{in}}(z) dz$$

$$= 2\pi\lambda_1 \int_0^{\infty} z \exp \left\{ -\frac{\tau}{P^m K_m} z^{a^m} \sigma^2 - \pi\lambda_1 z^2 + \widetilde{\mathcal{K}}_f(.) \right.$$

$$\left. -\lambda_d \pi (P_m^f K_m^f)^{\frac{2}{a^f}} x^{\frac{2*a^m}{a^f}} \right\} dz. \qquad (71)$$

Meanwhile, through (62), the theoretical value of Laplace transform has been considered as studied in related works [18]. We call the final result as approximate theoretical upper bound in this study, even it is close to the actual value due to the following considerations: 1) the value from the long-distance femtocell BSs will be very small, since it is proportional to d^{-a^f}, and 2) we consider all femtocell BSs are staying in a working status, based on huge communication requirements.

APPENDIX F
CALCULATING f_{xy}

In this section, we present the mathematical details of calculating f_{xy}. Based on (65), we have

$$f_{xy} = \int_{R^2} v(x+y) f(y) dy$$

$$= \int_{R^2} \frac{1}{1 + s_2 ||x+y||^{-a^f}} f(y) dy \qquad (72)$$

where $f(y)$ is the density function of the points in the cluster. Since for the Matern cluster process each point is uniformly distributed in a ball of radius D_c around the origin, the density function $f(y)$ is given by

$$f(y) = \begin{cases} \frac{1}{\pi D_c^2}, & ||y|| \le D_c \\ 0, & \text{otherwise}. \end{cases} \qquad (73)$$

Thus

$$f_{xy} = \int_{R^2} \frac{1}{1 + s_2 ||x+y||^{-a^f}} \frac{1}{\pi D_c^2} dy$$

$$= \mathbb{E}_y \left[\frac{1}{1 + s_2 (||x+y||)^{-a^f}} \right]$$

$$\overset{(i)}{\le} \frac{1}{1 + s_2 (\mathbb{E}_y [||x+y||])^{-a^f}} \quad (74)$$

where x is a parent point, y is a daughter point, and z is the location of the user. Step (i) is based on Jensen's inequality. Therefore

$$\mathbb{E}_y [||x+y||]_{y \le D_c} = 2\pi \int_0^{D_c} (x+y) y \frac{1}{\pi D_c^2} dy$$

$$= \left[\frac{2D_c}{3} + x \right]. \quad (75)$$

Finally, we obtain the following result:

$$f_{xy} \le \frac{1}{1 + s_2 \left(\left[\frac{2D_c}{3} + x \right] \right)^{-a^f}}. \quad (76)$$

APPENDIX G
SOLVING $\widetilde{\mathcal{K}}_f(.)$

In this section, we present the mathematical details for calculating $\widetilde{\mathcal{K}}_f(.)$, as defined in (68)

$$\widetilde{\mathcal{K}}_f(.) = -\frac{\mu * \lambda_c * 2\pi}{\mu + 1} \int_{\frac{2D_c}{3}}^{\infty} \left[\frac{t - \frac{2D_c}{3}}{[s_2(\mu+1)\mu^{-a^f}]^{-1} t^{a^f} + 1} \right] dt$$

$$\overset{(j)}{=} -\frac{\mu * \lambda_c * 2\pi}{\mu + 1} \left\{ \int_{\frac{2D_c}{3}}^{\infty} \frac{t}{Bt^{a^f}+1} dt - \int_{\frac{2D_c}{3}}^{\infty} \frac{\frac{2D_c}{3}}{Bt^{a^f}+1} dt \right\}. \quad (77)$$

In Step (j), $B = [s_2(\mu+1)\mu^{-a^f}]^{-1}$.

We let $Bt^{a^f} + 1 = v$, and obtain the following:

$$\int_{\frac{2D_c}{3}}^{\infty} \frac{t}{Bt^{a^f}+1} dt = \frac{(-1)^{\frac{2-a^f}{a^f}}}{a^f B^{\frac{2}{a}}} \int_{B(\frac{2D_c}{3})^{a^f}+1}^{\infty} v^{-1}(1-v)^{\frac{2-a^f}{a^f}} dv. \quad (78)$$

For simplicity, we let $\min = B(\frac{2D_c}{3})^{a^f} + 1$.

Furthermore, based on [42], (78) can be written as a hypergeometric function, as follows:

$$\int_{\frac{2D_c}{3}}^{\infty} \frac{t}{Bt^{a^f}+1} dt = \frac{1}{B^{\frac{2}{a}}(a^f-2) * \min^{\frac{a^f-2}{a^f}}}$$

$$* \cdot_2 F_1 \left(\frac{a^f-2}{a^f}, \frac{a^f-2}{a^f}; \frac{2*a^f-2}{a^f}; \frac{1}{\min} \right). \quad (79)$$

Similarly, $\int_{\frac{2D_c}{3}}^{\infty} \frac{\frac{2D_c}{3}}{Bt^{a^f}+1} dt$ can be written as follows:

$$\int_{\frac{2D_c}{3}}^{\infty} \frac{\frac{2D_c}{3}}{Bt^{a^f}+1} dt = \frac{\frac{2D_c}{3}}{B^{\frac{1}{a}}(a^f-1) * \min^{\frac{a^f-1}{a^f}}}$$

$$* \cdot_2 F_1 \left(\frac{a^f-1}{a^f}, \frac{a^f-1}{a^f}; \frac{2*a^f-1}{a^f}; \frac{1}{\min} \right). \quad (80)$$

Finally, we reach $\widetilde{\mathcal{K}}_f(.)$ as follows:

$$\widetilde{\mathcal{K}}_f(.) = -\frac{\mu * \lambda_c * 2\pi}{\mu + 1} \left\{ \int_{\frac{2D_c}{3}}^{\infty} \frac{t}{Bt^{a^f}+1} dt - \int_{\frac{2D_c}{3}}^{\infty} \frac{\frac{2D_c}{3}}{Bt^{a^f}+1} dt \right\}$$

$$= -\frac{\mu * \lambda_c * 2\pi}{(\mu + 1)} * \left\{ \frac{1}{B^{\frac{2}{a}}(a^f-2) * \min^{\frac{a^f-2}{a^f}}} \right.$$

$$* \cdot_2 F_1 \left(\frac{a^f-2}{a^f}, \frac{a^f-2}{a^f}; \frac{2a^f-2}{a^f}; \frac{1}{\min} \right)$$

$$- \frac{\frac{2D_c}{3}}{B^{\frac{1}{a}}(a^f-1) * \min^{\frac{a^f-1}{a^f}}}$$

$$\left. \times \cdot_2 F_1 \left(\frac{a^f-1}{a^f}, \frac{a^f-1}{a^f}; \frac{2a^f-1}{a^f}; \frac{1}{\min} \right) \right\}. \quad (81)$$

REFERENCES

[1] T. Sakano *et al.*, "Disaster-resilient networking: A new vision based on movable and deployable resource units," *IEEE Netw.*, vol. 27, no. 4, pp. 40–46, Jul. 2013.
[2] P. Yuan, Y. C. Liang, and G. Bi, "Dynamic access strategy selection in user deployed small cell networks," in *Proc. IEEE Wireless Commun. Netw. Conf.*, 2013, pp. 3649–3653.
[3] H.-Y. Hsieh, S.-E. Wei, and C.-P. Chien, "Optimizing small cell deployment in arbitrary wireless networks with minimum service rate constraints," *IEEE Trans. Mobile Comput.*, vol. 13, no. 8, pp. 1801–1815, Aug. 2014.
[4] W. Guo, S. Wang, X. Chu, J. Zhang, J. Chen, and H. Song, "Automated small-cell deployment for heterogeneous cellular networks," *IEEE Commun. Mag.*, vol. 51, no. 5, pp. 46–53, May 2013.
[5] H. S. Dhillon, R. K. Ganti, F. Baccelli, and J. G. Andrews, "Modeling and analysis of K -tier downlink heterogeneous cellular networks," *IEEE J. Sel. Areas Commun.*, vol. 30, no. 3, pp. 550–560, Apr. 2012.
[6] Y. Kim, S. Lee, and D. Hong, "Performance analysis of two-tier femtocell networks with outage constraints," *IEEE Trans. Wireless Commun.*, vol. 9, no. 9, pp. 2695–2700, Sep. 2010.
[7] Y. Tseng and C. Huang, "Analysis of Femto base station network deployment," *IEEE Trans. Veh. Technol.*, vol. 61, no. 2, pp. 748–757, Feb. 2012.
[8] R. Gonsalves, "Evaluation of outage probability in two-tier open access femtocell networks," in *Proc. Int. Conf. Circ. Syst. Commun. Inf. Technol. Appl.*, 2014, pp. 201–206.
[9] T. Morita, S. Tsukada, and A. Yuzawa, "Analysis of evacuation behaviors in different areas before and after the great east Japan earthquake," *Int. J.*, vol. 11, no. 25, pp. 2429–2434, 2016.
[10] S. N. Chiu, D. Stoya, W. S. Kendall, and J. Mecke, *Stochastic Geometry and Its Applications*, 3rd ed. Hoboken, NJ, USA: Wiley, 2013.

[11] Z. Jakó and G. Jeney, "Outage probability in poisson-cluster-based LTE two-tier femtocell networks," *Wireless Commun. Mobile Comput.*, vol. 15, pp. 2179–2190, 2014.

[12] J. Robinson and E. Knightly, "A performance study of deployment factors in wireless mesh networks," in *Proc. 26th IEEE Int. Conf. Comput. Commun.*, May 2007, pp. 2054–2062.

[13] W. Fu, X. Wang, and D. Agrawal, "Characterizing deployment and distribution of self-powered mesh routers in wireless mesh networks," in *Proc. IEEE 28th Int. Conf. Perform. Comput. Commun. Conf.*, Dec. 2009, pp. 185–192.

[14] T. Yan, Y. Gu, T. He, and J. A. Stankovic, "Design and optimization of distributed sensing coverage in wireless sensor networks," *ACM Trans. Embedded Comput. Syst.*, vol. 7, no. 3, 2008, Art. no. 33.

[15] C.-F. Huang, Y.-C. Tseng, and H.-L. Wu, "Distributed protocols for ensuring both coverage and connectivity of a wireless sensor network," *ACM Trans. Sensor Netw.*, vol. 3, no. 1, 2007, Art. no. 5.

[16] J. Cortes, S. Martinez, T. Karatas, and F. Bullo, "Coverage control for mobile sensing networks," *IEEE Trans. Robot. Autom.*, vol. 20, no. 2, pp. 243–255, Apr. 2004.

[17] H. Mahboubi, J. Habibi, A. Aghdam, and K. Sayrafian-Pour, "Distributed deployment strategies for improved coverage in a network of mobile sensors with prioritized sensing field," *IEEE Trans. Ind. Inform.*, vol. 9, no. 1, pp. 451–461, Feb. 2013.

[18] H.-s. Jo, Y. J. Sang, S. Member, P. Xia, J. G. Andrews, and S. Member, "Heterogeneous cellular networks with flexible cell association: A comprehensive downlink SINR analysis," *IEEE Trans. Wireless Commun.*, vol. 11, no. 10, pp. 3484–3495, Oct. 2012.

[19] J.-S. Wu, J.-K. Chung, and M.-T. Sze, "Analysis of uplink and downlink capacities for two-tier cellular system," in *IEEE Proc. Commun.*, vol. 144, no. 6, pp. 405–411, Dec. 1997.

[20] J. C. Ikuno, M. Wrulich, and M. Rupp, "System level simulation of LTE networks," in *Proc. IEEE 71st Veh. Technol. Conf.*, 2010, pp. 1–5.

[21] E. Ekici and C. Ersoy, "Multi-tier cellular network dimensioning," *Wireless Netw.*, vol. 7, no. 4, pp. 401–411, 2001.

[22] J. G. Andrews, F. Baccelli, and R. K. Ganti, "A tractable approach to coverage and rate in cellular networks," *IEEE Trans. Commun.*, vol. 59, no. 11, pp. 3122–3134, Nov. 2011.

[23] L. Gao, J. Acharya, and S. Gaur, "Heterogeneous networks–theory and standardization in LTE," *IEEE Wireless Commun. Netw. Conf. (IEEE WCNC2013)*, Shanghai, China, Apr. 7–10, 2013.

[24] H. S. Jo, Y. J. Sang, P. Xia, and J. G. Andrews, "Outage probability for heterogeneous cellular networks with biased cell association," in *Proc. IEEE Global Telecommun. Conf.*, 2011, pp. 1–5.

[25] S. Singh, H. S. Dhillon, and J. G. Andrews, "Offloading in heterogeneous networks: Modeling, analysis, and design insights," *IEEE Trans. Wireless Commun.*, vol. 12, no. 5, pp. 2484–2497, May 2013.

[26] H. Wang, X. Zhou, and M. C. Reed, "Coverage and throughput analysis with a non-uniform small cell deployment," *IEEE Trans. Wireless Commun.*, vol. 13, no. 4, pp. 2047–2059, Apr. 2014.

[27] J. Hoydis, A. Kammoun, J. Najim, and M. Debbah, "Outage performance of cooperative small-cell systems under Rician fading channels," in *Proc. IEEE 12th Int. Workshop Signal Process. Adv. Wireless Commun.*, 2011, pp. 551–555.

[28] H. Kalbkhani, M. G. Shayesteh, S. Jafarpour-Alamdari, and V. Solouk, "Outage probability of femtocells in two-tier networks with 6-sector macrocells," in *Proc. 6th Int. Symp. Telecommun.*, 2012, pp. 283–288.

[29] Y. Jiang, G. Yu, and R. Yin, "Genetic algorithm based access control in downlink open access small cell networks," in *Proc. 22nd Wireless Opt. Commun. Conf.*, May 2013, pp. 220–224.

[30] B. Ji, Z. Lu, K. Song, Y. Huang, and L. Yang, "The performance analysis and access mechanism of small cell network," in *Proc. IEEE 78th Veh. Technol. Conf.*, 2013, pp. 1–6.

[31] D. Vere-Jones, "Stochastic models for earthquake occurrence," *J. Roy. Statist. Soc. B*, vol. 32, pp. 1–62, 1970.

[32] M. Matsui, "Prediction in a poisson cluster model with multiple cluster processes," *Scand. Actuarial J.*, vol. 2015, no. 1, pp. 1–31, 2015.

[33] M. L. Thompson and P. Guttorp, "A probability model for severe cyclonic storms striking the coast around the Bay of Bengal," *Monthly Weather Rev.*, vol. 114, no. 11, pp. 2267–2271, 1986.

[34] M. Van Lieshout and A. Stein, "Earthquake modelling at the country level using aggregated spatio-temporal point processes," *Math. Geosci.*, vol. 44, no. 3, pp. 309–326, 2012.

[35] Y. Ogata, "Space-time point-process models for earthquake occurrences," *Ann. Inst. Statist. Math.*, vol. 50, no. 2, pp. 379–402, 1998.

[36] K. Hari, D. Baum, A. Rustako, R. Roman, and D. Trinkwon, "Channel models for fixed wireless applications," *IEEE 802.16 Broadband Wireless Access Working Group*, 2003.

[37] G. Miao, J. Zander, K. W. Sung, and S. B. Slimane, *Fundamentals of Mobile Data Networks*. Cambridge, U.K.: Cambridge Univ., 2016.

[38] M. K. Simon and M.-S. Alouini, *Digital Communication over Fading Channels*. Hoboken, NJ, USA: Wiley, 2005.

[39] H. S. Dhillon, R. K. Ganti, F. Baccelli, and J. G. Andrews, "Modeling and analysis of k-tier downlink heterogeneous cellular networks," *IEEE J. Sel. Areas Commun.*, vol. 30, no. 3, pp. 550–560, Apr. 2012.

[40] R. K. Ganti and M. Haenggi, "Interference and outage in clustered wireless ad hoc networks," *IEEE Trans. Inf. Theory*, vol. 55, no. 9, pp. 4067–4086, Sep. 2009.

[41] A. Baddeley, I. Bárány, and R. Schneider, "Spatial point processes and their applications," in *Stochastic Geometry*. New York, NY, USA: Springer, 2007, pp. 1–75.

[42] V. H. Moll, *Special Integrals of Gradshteyn and Ryzhik: The Proofs—Volume II*. Boca Raton, FL, USA: CRC, 2014.
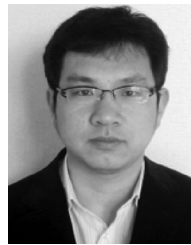
Junbo Wang (M'12) received the B.E. degree in electrical engineering and M.E. degree in computer science and engineering from Yanshan University, Qinhuangdao, China, and the Ph.D. degree in computer science and engineering from the University of Aizu, Aizuwakamatsu, Japan, in 2011.

He was a Postdoctoral Researcher with the IoT group in University of Aizu, from May 2011 to October 2012. After that, he joined the University of Aizu as an Associate Professor. He received research funding as Grant-in-Aid for Young Scientists from JSPS from 2013 to 2015 and is currently a Project Leader in a JST-NSF joint project to discuss big data for disaster. His research interests include Internet of Things, big data analytics, and emergency communication/information networks.

Dr. Wang is a member of the IEICE.
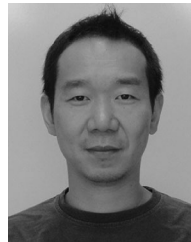
Song Guo (M'02–SM'11) received the Ph.D. degree in computer science from the University of Ottawa, Ottawa, ON, Canada.

He is currently a Full Professor with the Department of Computing, The Hong Kong Polytechnic University (HKPU), Hong Kong. Prior to joining HKPU, he was a Full Professor with the University of Aizu, Aizuwakamatsu, Japan. His research interests include mainly the areas of cloud and green computing, big data, wireless networks, and cyber-physical systems. He has published more than 300 conference and journal papers in these areas.

Dr. Guo is a senior member of ACM and an IEEE Communications Society Distinguished Lecturer. received multiple best paper awards from IEEE/ACM conferences. He has served as an editor of several journals, including the IEEE TRANSACTIONS ON PARALLEL AND DISTRIBUTED SYSTEMS, the IEEE TRANSACTIONS ON EMERGING TOPICS IN COMPUTING, the IEEE TRANSACTIONS ON GREEN COMMUNICATIONS AND NETWORKING, IEEE COMMUNICATIONS, and WIRELESS NETWORKS. He has been actively participating in international conferences as the General Chair and TPC Chair.

Zixue Cheng (M'95) received the M.S. and Ph.D. degrees in engineering from Tohoku University, Sendai, Japan, in 1990 and 1993, respectively.

He joined the University of Aizu, Aizuwakamatsu, Japan, in April 1993 as an Assistant Professor and has been a Full Professor since 2002. His research interests include design and implementation of protocols, distributed algorithms, distance education, ubiquitous computing, ubiquitous learning, embedded systems, functional safety, and the Internet of Things.

Dr. Cheng is a member of ACM, IEICE, and IPSJ.

Peng Li (S'10–M'12) received the B.S. degree from the Huazhong University of Science and Technology, Wuhan, China, in 2007, the M.S. and Ph.D. degrees in computer science from the University of Aizu, Aizuwakamatsu, Japan, in 2009 and 2012, respectively.

He is currently an Associate Professor with the University of Aizu. His research interests include networking modeling, cross-layer optimization, network coding, cooperative communications, cloud computing, smart grid, performance evaluation of wireless and mobile networks for reliable, energy-efficient, and cost-effective communications.

Jie Wu (F'16) received the B.S. degree in computer engineering, M.S. degree in computer science from Shanghai University of Science and Technology, and Ph.D. degree in computer engineering from, Florida Atlantic University.

He is the Associate Vice Provost for International Affairs at Temple University. He also serves as Director of Center for Networked Computing and Laura H. Carnell professor. He served as Chair of Computer and Information Sciences from 2009 to 2016. Prior to joining Temple University, he was a program director at the National Science Foundation and was a distinguished professor at Florida Atlantic University. His current research interests include mobile computing and wireless networks, routing protocols, cloud and green computing, network trust and security, and social network applications. He regularly publishes in scholarly journals, conference proceedings, and books.

Dr. Wu is a CCF Distinguished Speaker. He serves on several editorial boards, including IEEE Transactions on Service Computing and the Journal of Parallel and Distributed Computing. He was general cochair for IEEE MASS 2006, IEEE IPDPS 2008, IEEE ICDCS 2013, ACM MobiHoc 2014, ICPP 2016, and IEEE CNS 2016, as well as program cochair for IEEE INFOCOM 2011 and CCF CNCC 2013. He was an IEEE Computer Society Distinguished Visitor, ACM Distinguished Speaker, and chair for the IEEE Technical Committee on Distributed Processing (TCDP). He was the recipient of the 2011 China Computer Federation (CCF) Overseas Outstanding Achievement Award.